

^{23}Na NMR Chemical Shifts and Local Na Coordination Environments in Silicate Crystals, Melts and Glasses

Xianyu Xue* and Jonathan F. Stebbins**

Department of Geology, Stanford University, Stanford, CA 94305, USA

Received January 27, 1993 / Revised, accepted April 26, 1993

Abstract. In order to decipher information about the local coordination environments of Na in anhydrous silicates from ^{23}Na nuclear magnetic resonance spectroscopy (NMR), we have collected ^{23}Na magic angle spinning (MAS) NMR spectra on several sodium-bearing silicate and aluminosilicate crystals with known structures. These data, together with those from the literature, suggest that the ^{23}Na isotropic chemical shift correlates well with both the Na coordination and the degree of polymerization (characterized by NBO/T) of the material. The presence of a dissimilar network modifier also affects the ^{23}Na isotropic chemical shift. From these relations, we found that the average Na coordinations in sodium silicate and aluminosilicate liquids of a range of compositions at 1 bar are nearly constant at around 6–7. The average Na coordinations in glasses of similar compositions also vary little with Na content (degree of polymerization). However, limited data on ternary alkali silicate and aluminosilicate glasses seem to suggest that the introduction of another network-modifier, such as K or Cs, does cause variations in the average local Na coordination. Thus it appears that the average Na coordination environments in silicate glasses are more sensitive to the presence of other network-modifiers than to the variations in the topology of the silicate tetrahedral network. Further studies on silicate glasses containing mixed cations are necessary to confirm this conclusion.

Introduction

Alkali and alkaline earth elements (particularly Na, K, Mg, Ca) are important network-modifying cations in silicates of geological and technological interest. Among them, Na is relatively easy to study by NMR because the ^{23}Na nucleus has a 100% natural abundance and a high magnetogyric ratio. Many of the NMR studies

of sodium-bearing silicates and aluminosilicates (crystals, glasses and melts) have in fact included ^{23}Na NMR data. The line shapes of these spectra have often been discussed in terms of the number of Na sites, the dynamics of Na diffusion (e.g. Stebbins et al. 1985; Stebbins et al. 1989; Stebbins and Farnan 1992; Hovis et al. 1992), the structural order/disorder (e.g. Kirkpatrick et al. 1985; Jäger et al. 1989) or the distortion of the Na coordination (e.g. Buhl et al. 1988). There has been relatively less attention directed toward the structural significance of the ^{23}Na isotropic chemical shift (δ_i), compared to other NMR active nuclei in silicates such as ^{29}Si and ^{27}Al . This is partly because ^{23}Na is a quadrupolar nucleus with a spin quantum number of 3/2. The ^{23}Na NMR spectra are usually broadened by quadrupolar interactions and sometimes are featureless when there is structural disorder. In principle, the ^{23}Na δ_i should be sensitive to the local Na coordination environment. In a paper that derived formula for calculating MAS NMR line shapes of quadrupolar nuclei, including ^{23}Na , Kundla et al. (1981) reported ^{23}Na δ_i data for several aluminosilicates (mostly zeolites and sodalites) and pointed out that they cover a large range. In a multinuclear NMR study of alkali feldspar solid solution series, Phillips et al. (1988) also took note of the large ^{23}Na δ_i variation within this series and suggested that it is correlated with changes in the size of the Na sites. Oestrike et al. (1987) discussed ^{23}Na MAS NMR spectra of framework aluminosilicate glasses and suggested that ^{23}Na NMR has considerable potential to yield structural information for glasses. They also noted the need for a systematic study of the causes of variations in its δ_i .

In the first part of this paper, we investigate in detail the correlations between ^{23}Na δ_i and local structure around Na in anhydrous silicates and aluminosilicates. We first present ^{23}Na MAS NMR spectra and the derived NMR parameters for several crystalline sodium silicates and aluminosilicates with well-studied structures. Together with data for other crystalline phases in the literature, we discuss the various structural factors that affect the ^{23}Na δ_i .

* Now at: Earthquake Research Institute, Tokyo University, 1-1 Yayoi, Bunkyo-ku, Tokyo, 103 Japan

** To whom correspondence should be addressed

In the second part, we reexamine ^{23}Na NMR data for some anhydrous alkali silicate and aluminosilicate melts and glasses with the above results as a guide, and discuss the local Na environments in these phases. Up to now, information concerning the local Na environments in silicate glasses has mostly been derived from Na EXAFS and infra-red data. Greaves et al. (1981) have reported Na extended X-ray absorption fine structure (EXAFS) data for two silicate glasses ($\text{Na}_2\text{Si}_2\text{O}_5$ and $\text{Na}_2\text{CaSi}_5\text{O}_{12}$), from which they derived a Na coordination of 5 and Na–O distance of 2.3 Å for the $\text{Na}_2\text{Si}_2\text{O}_5$ glass and Na coordinations of 5 or 6 that are split in a similar way to crystalline ternary silicates for the $\text{Na}_2\text{CaSi}_5\text{O}_{12}$ glass. They suggested that Na adopts a similar variety of local structures in the glasses as it does in the crystalline phases. McKeown et al. (1985) have studied a number of sodium silicate and aluminosilicate glasses using Na EXAFS and X-ray absorption near-edge structure XANES. They concluded that the average Na coordination environments in these glasses are similar, with the Na coordinations range from 5.1 to 7.6 and the Na–O distances from 2.57 to 2.62 Å. The Na coordination number (6.4) and Na–O distance (2.61 Å) for a $\text{Na}_2\text{Si}_2\text{O}_5$ glass derived by McKeown et al. (1985) are, however, both larger than those of Greaves et al. (1981). More recently, Merzbacher and White (1988) have reported infra-red data for several sodium silicate and aluminosilicate glasses. They found that the vibrational energy of Na motions changes systematically with the degree of polymerization of the material and suggested that it indicates a change in the Na site structure, contrary to the conclusion of McKeown et al. (1985). There have also been several ^{23}Na NMR studies of sodium silicate and aluminosilicate melts (Stebbins et al.

1985, 1992) and glasses (Dupree et al. 1984; Oestrike et al. 1987; Hater et al. 1989; Xue et al. 1991), but unique interpretations of these spectra have been hampered by the lack of understanding of the correlations between ^{23}Na NMR parameters and the local Na structure. We will show that with the new information obtained in this study, we were able to gain more insight into the local Na coordination environments in sodium silicate melts and glasses from the ^{23}Na NMR data.

Experimental Procedure

All synthetic crystals were prepared by crystallizing glasses of the desired compositions. The starting glasses were prepared using reagent grade Na_2CO_3 , BaCO_3 and SiO_2 by the normal melt quench method described previously (Xue et al. 1991). The crystallization conditions of these crystals and the locality of a natural mineral are tabulated in Table 1. The identity and purity of all phases have been confirmed by powder X-ray diffraction and ^{29}Si MAS NMR. The ^{29}Si chemical shifts (Table 1) were calibrated against an external tetramethyl silane (TMS) standard and are accurate to about ± 0.2 ppm (see Xue et al. 1991 for details). The ^{29}Si chemical shifts of Na_2SiO_3 , $\alpha\text{-Na}_2\text{Si}_2\text{O}_5$ and jadeite are consistent with those previously reported (c.f. Engelhardt and Michel 1987). Those of $\beta\text{-Na}_2\text{Si}_2\text{O}_5$ and $\text{Na}_2\text{BaSi}_2\text{O}_6$ are reported here for the first time.

We have collected the ^{23}Na MAS NMR spectra using a Varian VXR-400S NMR spectrometer at a Larmor frequency of 105.8 MHz with a Doty Scientific, Inc., MAS probe. The liquid 90° pulse length measured on 1 M aqueous NaCl was about 5.4 μs . A short rf pulse length of 0.5–0.9 μs (about $17\text{--}30^\circ$ tip angle for the central transition in solids) was used to ensure quantitative and selective excitation of the central transitions of all Na sites. A delay time of 1 s was used for all samples. Samples were contained in a silicon nitride rotor with a 5 mm diameter. Sample spinning rates were about 8 to 11 kHz, which was enough to place

Table 1. Synthetic conditions or locality for crystalline samples, and ^{29}Si NMR data

Name	Composition	P, T conditions or locality	^{29}Si chemical shift (ppm)
sodium metasilicate	Na_2SiO_3	1 bar, 800°C	–76.8
sodium disilicate (α phase)	$\text{Na}_2\text{Si}_2\text{O}_5$	1 bar, 810°C	–94.2
sodium disilicate (β phase)	$\text{Na}_2\text{Si}_2\text{O}_5$	1 bar, 650°C^b	–86.3, –88.2 ^a
sodium barium metasilicate	$\text{Na}_2\text{BaSi}_2\text{O}_6$	1 bar, 800°C	–77.8, –75.2 ^a
jadeite	$\text{NaAlSi}_2\text{O}_6$	Clear Creek, Calif.	–91.8

^a Two peaks of equal intensity

^b The glass was first crystallized at about 0.2 Kbar and 600°C in a cold-seal vessel resulting in a mixture of β phase and phase C (a higher-pressure polymorph) and then was heated at 1 bar to eliminate phase C

Table 2. ^{23}Na NMR parameters of silicates and aluminosilicates obtained in this study

Phase	Na site	δ_i (ppm)	e^2qQ/h (MHz)	η	Relative Intensity
$\alpha\text{-Na}_2\text{Si}_2\text{O}_5$		16.9 ± 1.0	1.79 ± 0.1	1.0 ± 0.05	
$\beta\text{-Na}_2\text{Si}_2\text{O}_5$	Na(1)	15.6 ± 1.5	2.29 ± 0.1	0.85 ± 0.05	1
	Na(2)	9.4 ± 1.5	2.20 ± 0.1	0.55 ± 0.05	1
Na_2SiO_3		23 ± 3^a			
$\text{NaAlSi}_2\text{O}_6$ -jadeite		11.0 ± 1.0	3.30 ± 0.1	0.25 ± 0.05	
$\text{Na}_2\text{BaSi}_2\text{O}_6$	Na(1)	25.0 ± 1.0	2.10 ± 0.1	0.75 ± 0.05	1.0
	Na(2)	5.4 ± 1.0	2.96 ± 0.1	0.10 ± 0.05	1.5

^a Probably contains multiple Na sites, average value estimated

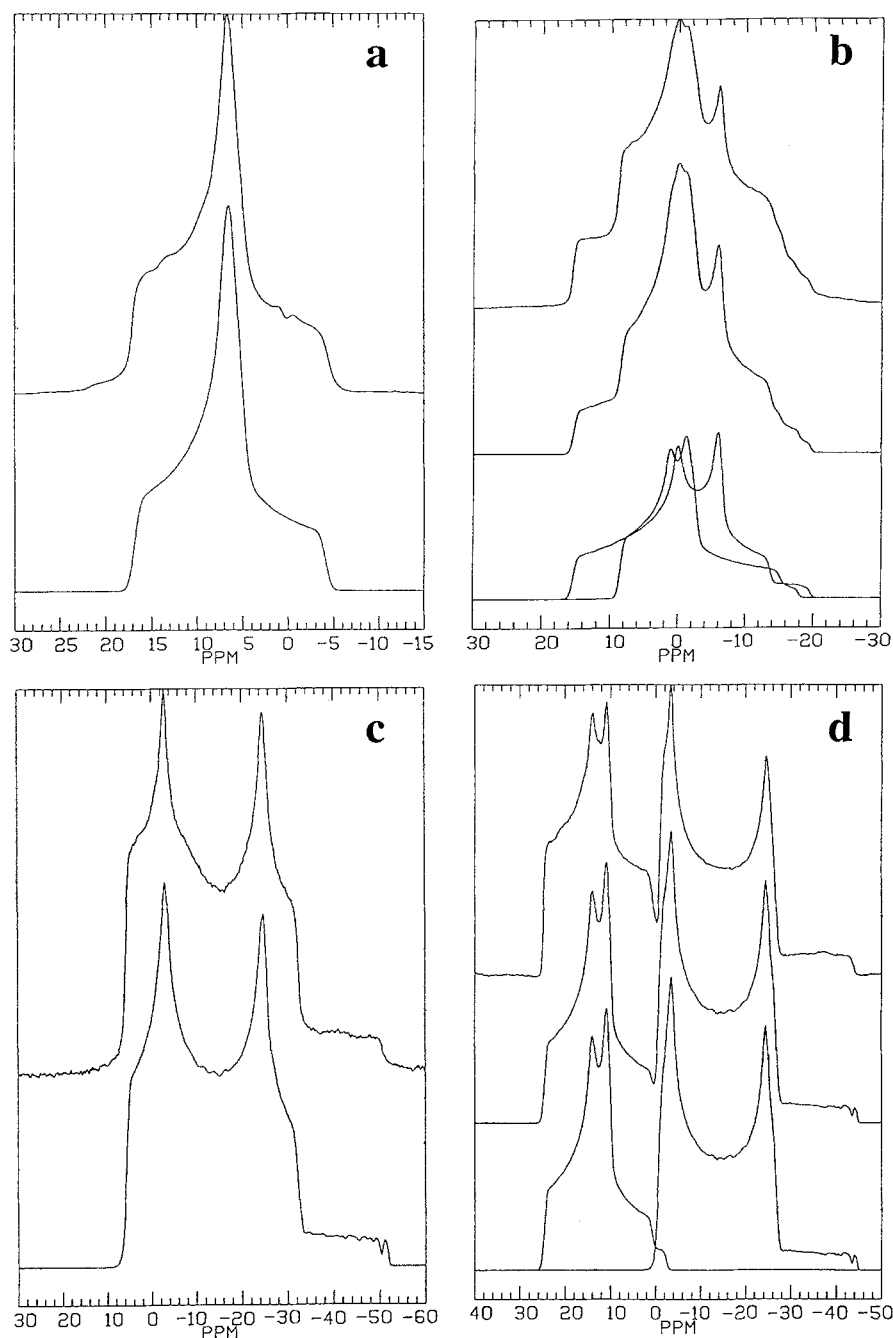


Fig. 1. ^{23}Na MAS NMR spectra and computer simulations of $\alpha\text{-Na}_2\text{Si}_2\text{O}_5$ (a); $\beta\text{-Na}_2\text{Si}_2\text{O}_5$ (b); $\text{Na}_2\text{BaSi}_2\text{O}_6$ (c); and $\text{NaAlSi}_2\text{O}_6$ jadeite (d). In each plot, the upper spectrum is the experimental spectrum and below it is the simulated spectrum. In (b) and (d), the components of the simulation are also shown at the bottom. All spectra were collected on 100–200 mg of sample with $0.9\ \mu\text{s}$ of pulse length, 1 s delay and 1000–7000 signal averages. The sample spinning rate for (a) was about 8 kHz, those of (b), (c) and (d) were about 11 kHz. No line broadening function was applied to the experimental spectra

the spinning side bands of the broadest peaks clear of the central peaks and thus allowed the spectra to be analyzed with an approximation of infinite spinning rate. The spectral width was usually 200 kHz and the digital resolution was 24 Hz. The probe deadtime and ringing time were about $15\ \mu\text{s}$ (equivalent to 3 points in the front of the FID, free induction decay). Frequencies were externally calibrated to about ± 0.4 ppm against 1 M NaCl solution. The ^{23}Na δ_i for the crystals have been derived from computer simulations of the MAS NMR spectra and thus have larger uncertainties that are quoted individually.

The algorithm used for the computer simulations was based on the formula derived by Müller (1982). In addition to δ_i , the simulation also yields the quadrupolar coupling constant (e^2qQ/h) and the asymmetry parameter (η) for each Na site. Because of the large spectral widths, the deadtime problem in general causes distortion of the spectra. The experimental spectra typically have slightly lower intensities in the center and more enhanced intensities

on either sides compared with the theoretical line shapes. The distortion is more severe for lines with large η , especially those in samples containing more than one Na sites, such as the $\text{Na}_2\text{BaSi}_2\text{O}_6$ phase (see Fig. 1). As a result, the best fits of the spectra were achieved by visual inspection to match the positions of discontinuities (e.g. peak maxima and shoulders), rather than by least squares minimization of the overall deviations of intensities, because these features are less affected by the distortions. Two of the phases ($\beta\text{-Na}_2\text{Si}_2\text{O}_5$ and $\text{Na}_2\text{BaSi}_2\text{O}_6$) studied here each contain two Na sites. For $\beta\text{-Na}_2\text{Si}_2\text{O}_5$, we were able to obtain a reasonable fit of the spectrum with two sites of equal intensity according to the structure (see Fig. 1 and Table 2). However for $\text{Na}_2\text{BaSi}_2\text{O}_6$, because of the different degrees of spectral distortions for the two Na sites due to their very different η and δ_i , we adjusted the relative intensity slightly ($\text{Na}(1):\text{Na}(2)=1:1.5$, instead of 1:1 as in the structure) in order to obtain a reasonable fit for both sites (see Fig. 1 and Table 2).

Results and Discussions

Silicate and Aluminosilicate Crystals

The experimental and simulated ^{23}Na MAS NMR spectra for the silicate and aluminosilicate crystals listed in Table 1 are shown in Figs. 1 and 2 and the simulation parameters are presented in Table 2. In Table 3 are also listed the ^{23}Na δ_i for a number of Na-bearing silicates and aluminosilicates from the literature. Because several different NaCl standards (NaCl solutions of various concentrations or solid NaCl) have been used in the literature, we have normalized all data to a common standard of 1 M NaCl solution (see Table 3 for details). We have restricted our compilation and subsequent discussions to anhydrous systems. The ^{23}Na δ_i of these silicates span a range of about 50 ppm.

The ^{23}Na MAS NMR spectra of α - and β - $\text{Na}_2\text{Si}_2\text{O}_5$, $\text{Na}_2\text{BaSi}_2\text{O}_6$, jadeite ($\text{NaAlSi}_2\text{O}_6$) (see Fig. 1) and low-albite ($\text{NaAlSi}_3\text{O}_8$) (Kirkpatrick et al. 1985; Phillips et al. 1988) all consist of one or two patterns with well defined quadrupolar line shapes in accordance with the crystal structures determined from X-ray or neutron diffraction, suggesting that there is no static disorder in the Na positions. For the Na_2SiO_3 phase, the ^{23}Na MAS NMR spectrum has three recognizable peak maxima (Fig. 2), suggesting that there are at least two Na sites. However, the crystal structure determined from x-ray diffraction contains only one Na site (McDonald and Cruickshank 1967). We have carefully checked our sample by powder x-ray diffraction and ^{29}Si MAS NMR (see Table 1), but found no other phases present. It is possible that the either Na positions in this phase are

partially disordered or that there is more than one crystallographically unique Na site. We have not attempted to obtain a satisfactory fit of the spectrum because of the lack of crystallographic constraints, but have estimated a mean δ_i value (see Table 2). The spectrum of anhydrous sodalite ($\text{Na}_6[\text{AlSiO}_4]_6$) (Buhl et al. 1988) has a poor signal-to-noise ratio and thus it is difficult to judge the order/disorder of the Na positions.

The spectrum of microcline ($(\text{Na}_{0.17}\text{K}_{0.83})\text{AlSi}_3\text{O}_8$) (see Phillips et al. 1988) does not have a well defined quadrupolar line shape, suggesting the presence of static disorder in the Na position. For silicates containing disordered K and Na distributions, such as microcline, X-ray diffraction data often gives only an average local structural for the alkalis residing in the same site. On the other hand, the NMR parameters for microcline may be considered as average values for Na (Phillips et al. 1988). In the subsequent discussions, we will directly compare the average Na/K structure from X-ray diffraction with the mean δ_i of Na cation. The underlying assumption is that the average environments of Na and K occupying the same site are close to each other, which may not be strictly valid and thus may introduce some uncertainties. The sodic nepheline ($\text{Na}_{0.75}(\text{Na}_{0.20}\text{K}_{0.05})\text{AlSiO}_4$) has two broad and featureless ^{23}Na MAS NMR peaks at room temperature as a result of static disorder of Na residing in each of the two alkali cages. At 200° C, however, the spectrum consists of two patterns with well defined quadrupolar line shapes, most likely due to motional averaging of the Na positional disorder within each alkali cage (Stebbins et al. 1989). The ^{23}Na δ_i listed in Table 3 are taken from simulations of the spectrum at 200° C (I. Farnan, personal communi-

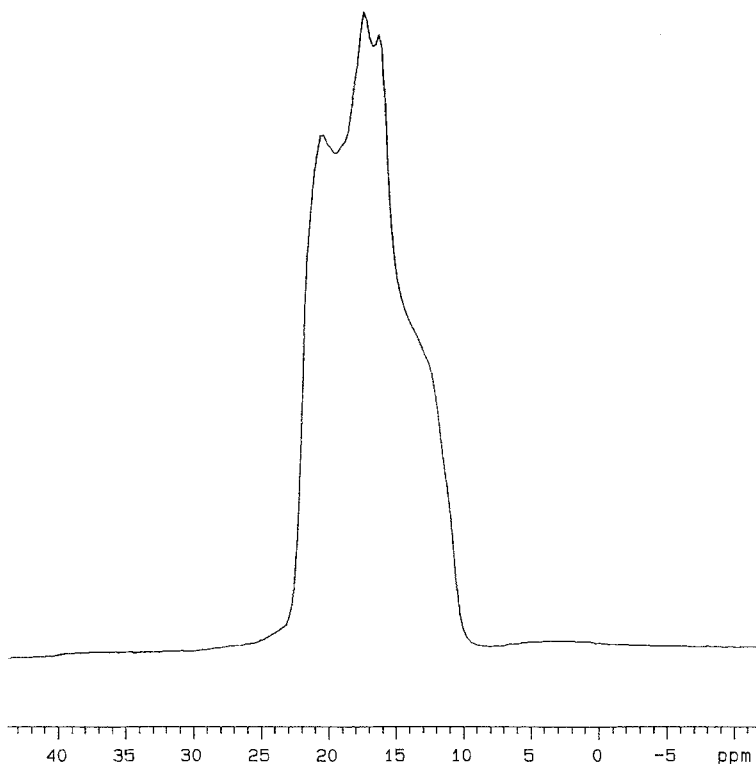


Fig. 2. ^{23}Na MAS NMR spectrum of crystalline Na_2SiO_3 . The spectrum was acquired on about 100 mg of sample with 0.5 μs of pulse length, 1 s delay and 100 signal averages. The sample spinning rate was about 8 kHz. No line broadening function was applied to the experimental spectra

Table 3. ^{23}Na NMR isotropic chemical shifts and structural parameters of anhydrous silicate and aluminosilicate crystals and liquids

Phase	Na site	NBO/T	σ_i (ppm)	Corr. σ_i^a (ppm)	Original NMR std.	$N_{\text{Na-O}}^b$	$d_{\text{Na-O}}^b$		$\sum v_{\text{Na-O}}^c$	NMR reference	Structure reference
							(Å)	(Å)			
<i>Crystals</i>											
$\text{Na}_2\text{Si}_2\text{O}_5-\alpha$		1	16.9 ± 1	16.9	1 M NaCl	5	2.40	1.04	1		9
$\text{Na}_2\text{Si}_2\text{O}_5-\beta$	Na(1)	1	15.6 ± 1.5	15.6	1 M NaCl	5	2.42	0.98	1		10
	Na(2)	1	9.4 ± 1.5	9.4	1 M NaCl	6	2.45	1.03	1		10
Na_2SiO_3		2	23 ± 3	23	1 M NaCl	5	2.38	1.07	1		11
$\text{Na}_2\text{BaSi}_2\text{O}_6$	Na(1)	2	25.0 ± 1	25	1 M NaCl	5	2.35	1.16	1		12
	Na(2)	2	5.4 ± 1	5.4	1 M NaCl	8	2.74	0.84	1		12
$\text{NaAlSi}_2\text{O}_6$ jadeite		2	11.0 ± 1	11.0	1 M NaCl	8	2.47	1.42	1		13
$\text{Na}_{0.75}(\text{Na}_{0.20}\text{K}_{0.05})\text{AlSiO}_4$ nepheline	Na site	0	-5.5	-5.5	1 M NaCl					2 ^d	14
	K site	0	-19.5	-19.5	1 M NaCl					2 ^d	14
$\text{NaAlSi}_3\text{O}_8$ albite		0	-8.5	-8.5	1 M NaCl	8	2.71	0.89	3		15
		0	-6.8 ± 0.3	-6.6	3 M NaCl	8	2.71	0.89	4		15
		0	-7.3 ± 2.0	-7.1	3 M NaCl	8	2.71	0.89	5		15
		0	-24.3	-24.3	1 M NaCl	10	3.01	0.43	3		16 ^e
$(\text{Na}_{0.17}\text{K}_{0.83})\text{AlSi}_3\text{O}_8$ microcline		0	-24.3	-24.3	1 M NaCl	10	3.01	0.43	3		16 ^e
$\text{Na}_6[\text{AlSiO}_4]_6$ anhydrous sodalite		0	-9 ± 4	-1.7	solid NaCl	6	2.63	0.41	6		17
<i>Liquids</i>											
Na_2SiO_3 (1100° C)		2	$13 (2.5)^f$	13.7	6.5 M NaCl						7
$\text{Na}_2\text{Si}_2\text{O}_5$ (1100° C)		1	$7 (5)^f$	7.7	6.5 M NaCl						7
$35\text{Na}_2\text{O} \cdot 15\text{Al}_2\text{O}_3 \cdot 50\text{SiO}_2$ (1100° C)		0.5	$5(6)^f$	5.7	6.5 M NaCl						7
$\text{NaAlSi}_2\text{O}_6$ (1100° C)		0	$-4.4 (16)^f$	-3.7	6.5 M NaCl						7
$31.3\text{Na}_2\text{O} \cdot 6.2\text{Al}_2\text{O}_3 \cdot 62.5\text{SiO}_2$ (1050° C)		0.67	4	4	1 M NaCl						8
$31.3\text{Na}_2\text{O} \cdot 6.2\text{Al}_2\text{O}_3 \cdot 62.5\text{SiO}_2$ (1350° C)		0.67	3	3	1 M NaCl						8

^a Chemical shifts relative to 1 M NaCl solution; the correction scheme follows Templeman and Van Geet (1972). Specifically, 0.2 ppm is added to those relative to 3 M NaCl; 0.7 ppm added to those relative to 6.5 M NaCl; and 7.3 ppm added for those relative to solid NaCl (assuming the shift of solid NaCl relative to 3 M NaCl is 7.1 ppm following Kundla et al. (1981))

^b Na coordination and average Na—O bond distance

^c Bond valence sum

^d The data are simulations of the spectrum measured at 200° C and were provided by I. Farnan (per. commun.)

^e Data for sample CA1E (Or89)

^f Numbers in the brackets are line widths

References: 1. this work; 2. Stebbins et al. (1989); 3. Phillips et al. (1988); 4. Kirkpatrick et al. (1985); 5. Kundla et al. (1981); 6. Buhl et al. (1988); 7. Stebbins et al. (1985); 8. Stebbins et al. (1992); 9. Pant & Cruickshank (1968); 10. Pant (1968); 11. McDonald and Cruickshank (1967); 12. Gunawardane et al. (1973); 13. Prewitt and Burnham (1966); 14. Dallase and Thomas (1978); 15. Harlow and Brown (1980); 16. Dal Negro et al. (1978; 1980); 17. Felsche et al. (1986)

cation), and may be considered to correspond to the average environments for each of the two Na sites at this temperature. However, because of the lack of accurate information about its average structure at elevated temperature, we will exclude the data for nepheline in the subsequent discussions.

Before we discuss the correlations between ^{23}Na δ_i and local Na coordination environments, it is necessary to examine the concept of Na coordination for silicates. The Na—O bonds are more ionic and much weaker than Si—O or Al—O bonds and the Na coordinations are thus often believed to be ill-defined. Figure 2 shows the number of oxygens as a function of distance from the central Na up to 4.0 Å for the phases under discussion. The Na sites in Na_2SiO_3 , α - and β - $\text{Na}_2\text{Si}_2\text{O}_5$, and anhydrous sodalite, as well as the Na(1) site in $\text{Na}_2\text{BaSi}_2\text{O}_6$ (Fig. 3) all have well defined first coordination spheres of 5 or 6 oxygens, i.e. the more distant oxygens are well separated by about 1 Å or more from the first coordination sphere. In jadeite, there are six oxygens at distances within 2.41 Å and two others at 2.74 Å, and the more distant oxygens are further separated from these by about 0.6 Å (Fig. 3). Thus the Na site in jadeite may be considered to be 8-coordinated. The alkali site in mi-

crocline has a continuous distribution of 10 oxygens up to 3.4 Å and there is a gap of about 0.5 Å from the more distant oxygens (Fig. 3) and thus the Na in this site may be considered 10-coordinated. However, for the Na(2) site in $\text{Na}_2\text{BaSi}_2\text{O}_6$, there is a continuous distribution of oxygens all the way to 3.98 Å (within the 4.0 Å limit). For the Na site in albite, there is also a continuous distribution of oxygen all the way to 3.74 Å. Therefore, for Na coordinations below 8 in the compounds considered here, there is a clear distinction between the first and outer oxygen coordination spheres and thus there is no ambiguity with the concept of Na coordination. But for larger Na sites, as pointed out by Phillips et al. (1988), the coordination number of Na is to some extent arbitrary. It is conceivable that the effective distance within which oxygens can be considered to be bonded to Na also depends on the sensitivity of the technique in question. For the Na site in albite and the Na(2) site in $\text{Na}_2\text{BaSi}_2\text{O}_6$, we will use 3.4 Å as the cutoff distance, which is roughly the dividing point for the oxygens in the first coordination spheres and the more distant oxygens in the phases discussed above. This results in a coordination of 8 for both Na sites. It should be kept in mind that for some Na sites, such as the Na(2)

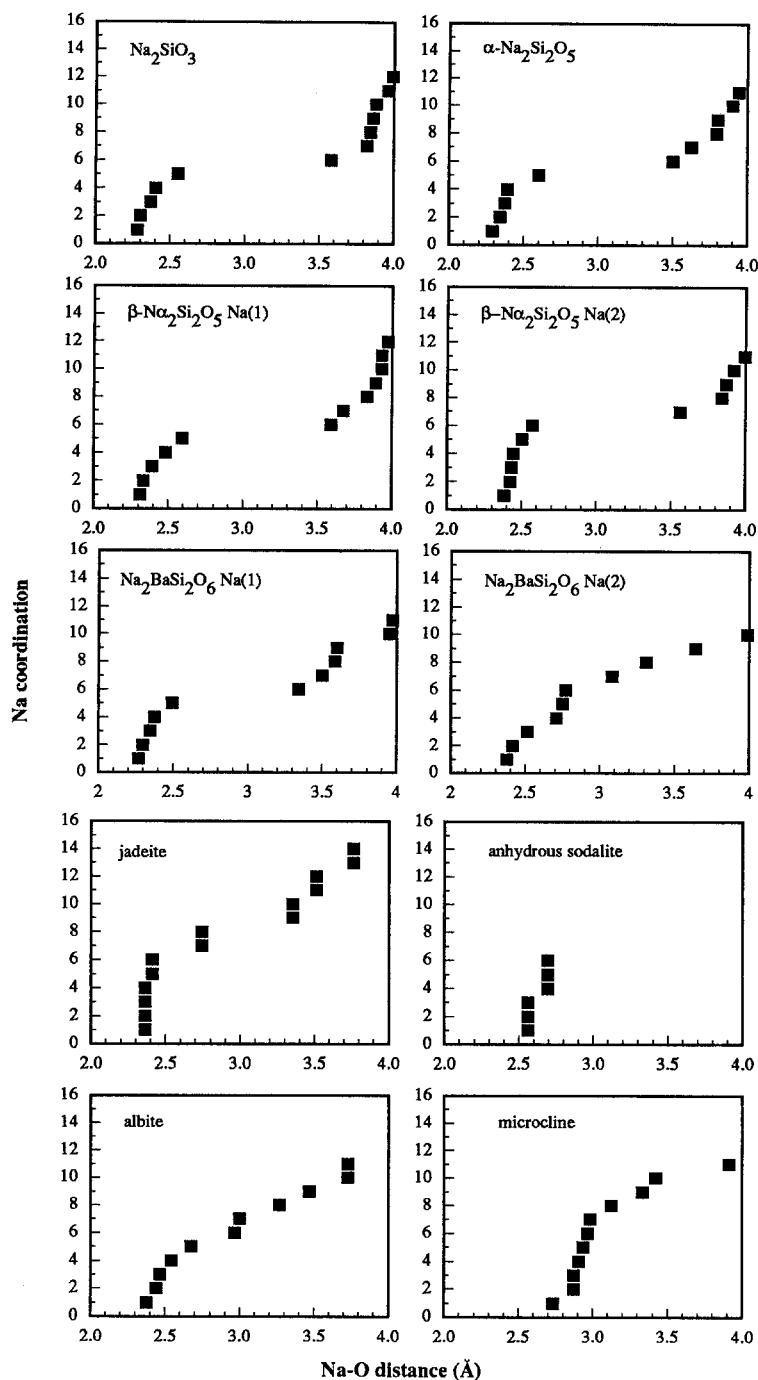


Fig. 3. Na coordination versus Na–O distance up to 4 Å for Na sites in Na_2SiO_3 , α - and β - $\text{Na}_2\text{Si}_2\text{O}_5$, $\text{Na}_2\text{BaSi}_2\text{O}_6$, jadeite, anhydrous sodalite, albite and microcline. The structural references are tabulated in Table 3

site in $\text{Na}_2\text{BaSi}_2\text{O}_6$, the Na coordination numbers defined in this way are larger than normally described in the crystallographic literature.

The ^{23}Na δ_i values are plotted against the Na coordination number and against the mean Na–O distance in Fig. 4. In general, the data show a trend of decreasing δ_i with increasing Na coordination and increasing mean Na–O bond distance. Decreasing δ_i with increasing Na coordination has also been observed for Na in sodium aluminofluorides (Dirken et al. 1992; Stebbins et al. 1992). This trend is consistent with that observed for other cation nuclei such as ^{29}Si and ^{27}Al , and reflects the lower electron density around the cation with in-

creasing coordination (and accordingly increasing mean cation–oxygen distance). However, there is considerable scatter in the plot of ^{23}Na δ_i vs. Na coordination (Fig. 4a). The δ_i of Na sites with different coordinations overlap. The same can be seen for ^{23}Na δ_i of sodium aluminofluorides (Dirken et al. 1992; Stebbins et al. 1992). While part of the scatter may be related to the arbitrariness of the Na coordinations, the large scatter, even for the low Na coordination numbers that are well defined, suggests that there are other factors that significantly affect ^{23}Na δ_i .

In contrast to known trends for ^{29}Si or ^{27}Al , the scatter in the relation between ^{23}Na δ_i and Na coordina-

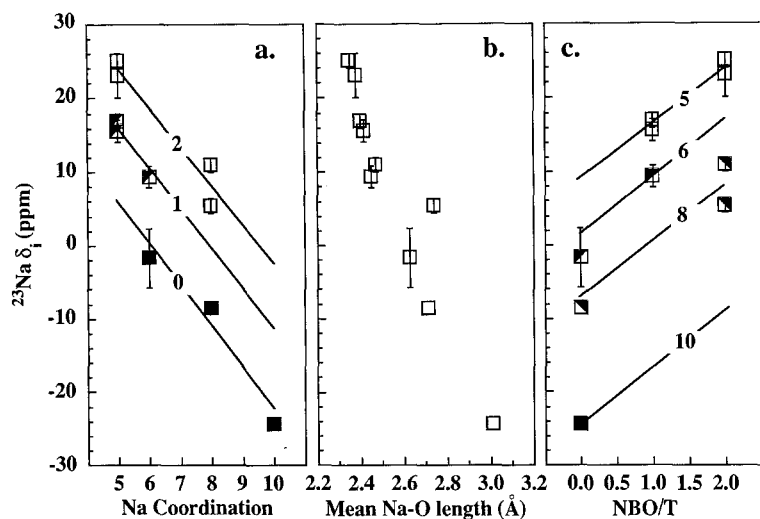
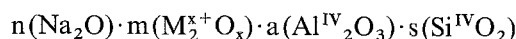


Fig. 4. **a** ^{23}Na δ_i versus Na coordination number. Numbers on the lines refer to the NBO/T (non-bridging oxygens per tetrahedral cation) of the crystals. Different symbols denote different NBO/T; **b** ^{23}Na δ_i versus mean Na–O distance; **c** ^{23}Na δ_i versus NBO/T. Numbers on the line are Na coordination numbers. Different symbols represent different Na coordination numbers. Wherever available, the error bars for the ^{23}Na δ_i are also shown. All data are for anhydrous silicate and aluminosilicate crystals tabulated in Table 3

tion cannot be attributed to the effect of second neighbor cations (the cations bonded to the first neighbor oxygens). For example, the Na sites in both Na_2SiO_3 and $\alpha\text{-Na}_2\text{Si}_2\text{O}_5$ (both 5-coordinated) have four nonbridging oxygen and one bridging oxygen neighbors, despite the large difference in their ^{23}Na δ_i . This lack of correlation with second neighbor cation is not surprising considering that the Na–O bonds are much weaker than the Si–O or Al–O bonds.

On the other hand, for a given Na coordination number, there is a clear general trend of increasing ^{23}Na δ_i with increasing degree of polymerization of the structure. In Fig. 4c we have plotted ^{23}Na δ_i as a function of NBO/T (nonbridging oxygens per tetrahedrally coordinated cation), which is a measure of the degree of polymerization of silicates. The NBO/T for a material with a general formula of



can be calculated as following:

$$\text{NBO/T} = 2(n + mx - a)/(2a + s)$$

where M is a network modifier other than Na; Al^{IV} and Si^{IV} are tetrahedrally coordinated Al and Si, respectively; and n, m, a and s are the mole fractions of the respective oxide components. Note that six-coordinated Al (Al^{VI}), as in jadeite, would be classified as a network-modifier. This correlation between chemical shift and structure is clear for at least 5, 6, and 8-coordination, and we might expect parallel lines for other Na coordinations as well. The data thus map out iso-coordination contours (Fig. 4c). Similarly, for the ^{23}Na δ_i vs. Na coordination plot in Fig. 4a, by grouping the data according to NBO/T, there is a better trend of decreasing δ_i with increasing Na coordination.

Interestingly, increasing NBO/T roughly correlates with increasing number of first neighbor Na ions around a central Na for sodium silicate crystals. With a cutoff distance of 3.5–3.6 Å (that seems in these sodium silicates to be a natural break point beyond which there is a relatively large interval that has no Na neighbors), the number of Na neighbors is 7 for the Na site in $\text{Na}_2\text{-}$

SiO_3 (NBO/T=2), 4 for Na sites in α - and β - $\text{Na}_2\text{Si}_2\text{O}_5$ (NBO/T=1), and 0 for Na sites in fully polymerized aluminosilicates such as albite and microcline (NBO/T=0). Because the shortest Na–Na distances in alkali silicates are about 3.1 Å, which are only moderately longer than the Na–O distances, these Na ions may be considered to be clustered. The clustering (microsegregation) of alkali ions in alkali silicate glasses has also been noted recently by Vessal et al. (1992) from molecular dynamics simulations. We may expect that the interactions among Na within the cluster have a significant effect on ^{23}Na σ_i and that the correlation between ^{23}Na δ_i and NBO/T may actually be related to the number of first neighbor network modifiers. An increase in the number of first neighbor network-modifiers (and accordingly an increase in NBO/T) may result in a decrease in the positive charge on the central Na (higher electron density) and thus an increase in its δ_i . The effects of this direct interaction of Na with its neighboring network-modifiers is in contrast to what is observed for ^{29}Si and ^{27}Al NMR spectra. For the smaller, more highly charged Si and Al cations, first neighbor cations are generally considered to influence chemical shifts through modification of the electron distributions around the intervening oxygens (c.f. Kirkpatrick 1988). This difference in behavior may account for the greater relative effect of first neighbor anion coordination (relative to that of first neighbor cation coordination) for these nuclides when compared to ^{23}Na .

Nevertheless, because the parameter NBO/T can be calculated without detailed structural information, it is more useful in practice for interpreting the ^{23}Na δ_i for unknown structures than the number of first neighbor cations. Fig. 4c can be used to predict the coordination of Na in unknown silicate phases from the ^{23}Na δ_i . It is also worth noting the relatively tight correlations between the ^{23}Na δ_i and the mean Na–O distance (Fig. 4b). This may be accounted for by the fact that the mean Na–O distance is correlated with both the Na coordination and the NBO/T of the material.

The presence of network modifiers other than Na also seems to affect ^{23}Na δ_i . The difference in the δ_i

(about 5 ppm) between Na(2) in $\text{Na}_2\text{BaSi}_2\text{O}_6$ and Na in jadeite (both with $\text{NBO}/\text{T}=2$, Na coordination of 8) may be largely caused by the difference in the type of the second network modifier (Ba vs. Al^{VI}). This may again be the result of first neighbor cation interactions (between Na and its neighboring dissimilar network modifiers), similar to the effect of the number of neighboring network modifiers discussed above. The higher field strength of Al^{VI} causes proportionally lower positive charge (and accordingly higher electron density) around Na and thus larger δ_i and vice versa for Ba.

A parameter that is a useful measure of the electron density around Na is the bond valence sum for the Na–O bonds ($\sum v_{\text{Na-O}}$), which is a function of both the Na–O bond lengths and the Na coordination number. The bond valence sum for a give ion in solids is expected to be close to its formal charge, although in reality, there are some deviations, especially for alkalis (c.f. Brown and Altermatt 1985; Brese and O’Keeffe 1991). A common definition of the bond valence is

$$v_{ij} = \exp [R_{ij} - d_{ij}/b]$$

where b is a universal constant, d_{ij} is the bond distance between ion pair i and j , and R_{ij} is a constant for the ion pair that has been compiled from crystal structure information (see Brown and Altermatt 1985; Brese and O’Keeffe 1991 and references therein). Using $R_{\text{Na-O}}$ of 1.80 and b of 0.37 Å following Brese and O’Keeffe (1991), we have calculated $\sum v_{\text{Na-O}}$ for the phases examined in this study (Table 3). The results indeed suggest that in jadeite Na is significantly overbonded (with a $\sum v_{\text{Na-O}}$ of 1.42), whereas in the Na(2) site of $\text{Na}_2\text{BaSi}_2\text{O}_6$, Na is underbonded (with a $\sum v_{\text{Na-O}}$ of 0.84). The δ_i of the Na(1) site in $\text{Na}_2\text{BaSi}_2\text{O}_6$ and the Na site in Na_2SiO_3 (both 5-coordinated with a NBO/T of 2) are similar, suggesting that this effect is only dramatic when the dissimilar network-modifiers have very different field strengths. We may postulate in general that in silicates with mixed network modifiers, one of which has a much higher field strength than Na (such as Al, Zr, Ti), the ^{23}Na δ_i would be higher than the trends defined by pure sodium silicates and aluminosilicates in the ^{23}Na δ_i vs. Na coordination plot. Following the same reasoning, we may predict that in silicates with mixed four- and six-coordinate Si, the ^{23}Na δ_i would be even higher than such trends.

In summary, a major influence on the ^{23}Na δ_i of anhydrous silicates and aluminosilicates is the first neighbor anion effect, i.e. the Na coordination number and the Na–O bond distance. There is a general trend of decreasing ^{23}Na δ_i with increasing Na coordination and increasing mean Na–O bond length. With a constant NBO/T and in the absence of other types of network-modifiers, the difference seems to be on the order of 30 ppm from 5- to 10-coordination. However, other factors cause overlap of the ^{23}Na δ_i for different NA coordinations, in contrast to ^{29}Si NMR. Another parameter that has a large effect on the ^{23}Na δ_i is the bulk NBO/T . The ^{23}Na δ_i decreases by about 15 ppm from NBO/T of 2 to 0 at a constant Na coordination. This effect may also be related to the number of net-

work-modifiers around the central Na and thus may be considered as a first neighbor cation effect. In addition, the presence of dissimilar network modifiers also affects the ^{23}Na δ_i . A sodium silicate containing Ba as the second network modifier has a smaller ^{23}Na δ_i than that containing a higher field strength cation Al^{VI} (by about 5 ppm). This effect may be related to the type of the first neighbor network modifiers.

Silicate and Aluminosilicate Melts and Glasses

In Table 3, we have also compiled ^{23}Na NMR data for sodium silicate and aluminosilicate liquids at 1050–1350° C obtained by Stebbins et al. (1985; 1992). All these systems contain only Na as the network-modifier. At the experimental temperatures, the rapid motions of atoms cause narrowing and coalescence of the NMR lines and the center of the line can be considered as the mean δ_i . All except the $\text{NaAlSi}_2\text{O}_6$ melt indeed have very narrow ^{23}Na NMR lines (≤ 6 ppm) (Table 3). The $\text{NaAlSi}_2\text{O}_6$ melt has a larger width of about 12 ppm (Table 3), which may be caused by rapid quadrupolar relaxation.

Plotted in Fig. 5 is the ^{23}Na δ_i vs. NBO/T for these melts as well as for the crystals, as in Fig. 4c. Because it has been well documented that Al in these melts is essentially tetrahedrally coordinated, we have included all the Al in the T term of NBO/T . The data for all these melts fall more or less on a line parallel to the iso-coordination lines (Fig. 5), suggesting that they have similar average local Na environments. The average Na coordination can be estimated to be about 6–7 from the plot. The relatively small variations in the average Na environments in melts of diverse compositions, as opposed to the large variations in crystals, may be relat-

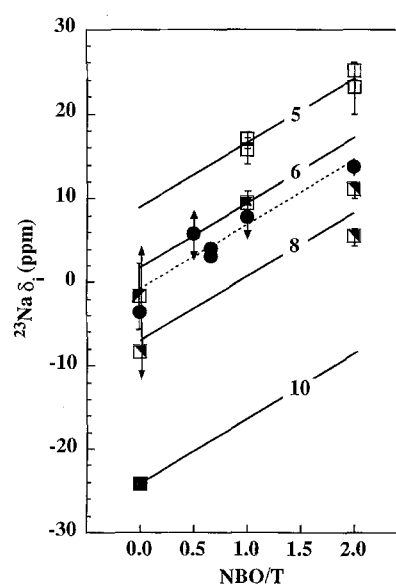


Fig. 5. ^{23}Na δ_i versus NBO/T for sodium silicate and aluminosilicate crystals and melts. The data and symbols for the crystals (squares) and the iso-coordination lines are the same as in Fig. 4(c). Data for the melts (filled circles) are tabulated in Table 3. Arrows on the data points of the melts indicate line widths, not errors. The dashed line is a guide for the data points of the melts

ed to the flexible structure of disordered liquids. In a crystalline phase, the geometry of the Na sites is to a large extent controlled by the SiO_4 (and AlO_4) network. In contrast, we may expect more freedom in the liquid structure and thus Na may be in a more ideal and constant geometry. The lack of large changes in the average local environments of Na (and possibly some other alkalis as well) in silicate melts with composition may be responsible for the relatively insignificant role of melt composition in the partitioning of some alkali and alkaline earth elements between minerals (e.g. feldspar) and melts (see Blundy and Wood 1991; 1992 and references therein).

These NMR data also suggest that the average Na coordination environments in melts are also relatively insensitive to temperature. The average ^{23}Na δ_i of the melt with a composition of $31\text{Na}_2\text{O} \cdot 6\text{Al}_2\text{O}_3 \cdot 63\text{SiO}_2$ is about 3 ppm at 1350°C , and increases by only about 1 ppm with a temperature drop of 300°C (Stebbins and Farnan 1992); also see Table 3). If roughly extrapolated to near its glass transition temperature (about $400\text{--}500^\circ\text{C}$) assuming a linear change with temperature, the mean δ_i would further increase by <2 ppm. Thus we might expect similar average Na coordination environments in the glass and in the liquid.

We have reported ^{23}Na MAS NMR spectra for glasses of $\text{Na}_2\text{Si}_2\text{O}_5$ and $\text{Na}_2\text{Si}_4\text{O}_9$ compositions quenched from liquids at pressures up to 8 GPa (at a Larmor frequency of 105.8 MHz as in this study) in Xue et al. (1991). As discussed previously, the lack of characteristic quadrupolar line shapes and the large widths of

the spectra suggest the presence of a range of δ_i and/or quadrupolar coupling parameters, as expected from a disordered phase. A conspicuous feature of these spectra is the relatively small change with either composition or pressure. There is a slight shift (2–3 ppm) of the peak maximum to higher frequency from the Na_2SiO_5 to the $\text{Na}_2\text{Si}_4\text{O}_9$ glass. A similar trend was also observed previously for glasses of a broader range of compositions in the $\text{Na}_2\text{O} \text{--} \text{SiO}_2$ binary (Dupree et al. 1984). The extent of change in the peak maximum with composition is similar to that observed in the liquids of comparable compositions and may thus be a simple result of increasing mean δ_i due to increased polymerization of the material. Thus as in the liquid, the average Na environments in these glasses appears to vary little with composition. For both compositions, the main spectral change with pressure from 1 bar to 8 GPa is a slight decrease in the line width. Interpretation of these spectra are more complicated. The presence of Si^{VI} in the glasses quenched from 8 GPa may cause the ^{23}Na δ_i to shift toward higher frequency even at a constant Na coordination, as discussed above. On the other hand, it has been predicted from molecular dynamics simulations that the average Na coordination number in $\text{Na}_2\text{Si}_2\text{O}_5$ liquid increases with pressure within a similar pressure range (M. Kanzaki, personal communication.), which would correspond to a shift of the NMR peak to the opposite direction. It is also conceivable that because of the broadness of these spectra, ^{23}Na NMR of glasses are less sensitive to small changes in the Na environments than are those of crystals or liquids.

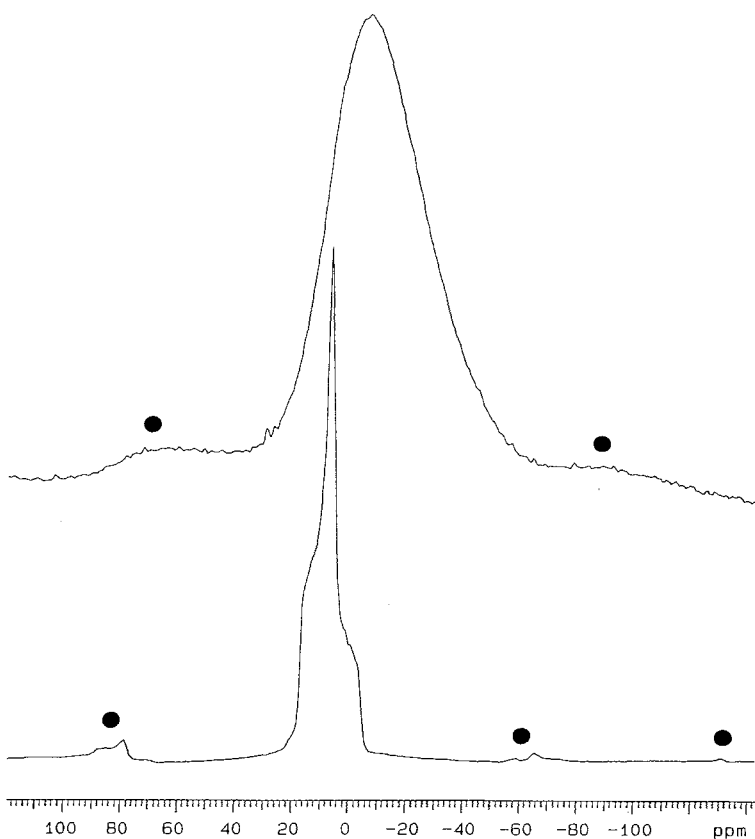


Fig. 6. Comparison of ^{23}Na MAS NMR spectra of a $\text{Na}_2\text{Si}_2\text{O}_5$ glass quenched from liquid at 1 bar (*upper*) and that of $\alpha\text{-Na}_2\text{Si}_2\text{O}_5$ (*lower*). The spectrum for the glass has been described in Xue et al. (1991) and that of the α phase is identical to Fig. 1a. Spinning sidebands are marked by dots

In Fig. 6 we compare the ^{23}Na MAS NMR spectra of the $\text{Na}_2\text{Si}_2\text{O}_5$ glass quenched from liquid at 1 bar with that of $\alpha\text{-Na}_2\text{Si}_2\text{O}_5$. The peak maximum of the glass is significantly displaced to lower frequency relative to that of the α phase (in which Na is five-coordinated), which may be caused by an increase in the mean δ_i and/or an increase in the mean quadrupolar coupling constant. The former is consistent with the conclusion derived from the NMR data of $\text{Na}_2\text{Si}_2\text{O}_5$ melt.

McKeown et al. (1985) have conducted EXAFS studies for sodium silicate and aluminosilicate glasses of several compositions and found that the Na coordinations are relatively constant, consistent with the NMR results. The coordination numbers they obtained (5.1–7.6) are also close to our results for melts of similar compositions, although in a similar EXAFS study, Greaves et al. (1981) obtained a lower Na coordination number (5) for a $\text{Na}_2\text{Si}_2\text{O}_5$ glass. In a recent infra-red study of sodium silicate and aluminosilicate glasses, Merzbacher and White (1988) found that the vibrational energy of Na motions changes systematically with the degree of polymerization of the system. They attributed this change in vibrational energy to a change in the Na site structure, which is apparently inconsistent with the EXAFS results of McKeown et al. (1985) or the NMR results. A possible explanation for such an apparent discrepancy could be that the change in the vibrational energy with polymerization of the system may actually reflect changes in the interactions among network-modifiers, because such interactions change systematically with polymerization as discussed earlier in connection with ^{23}Na δ_i . It is not necessarily an indication of the Na coordination change. EXAFS, on the other hand, is more sensitive to the local geometry of the Na environments (Na coordinations). ^{23}Na NMR is sensitive to both effects.

Hater et al. (1989) also reported ^{23}Na MAS NMR results on mixed alkali (Na and Cs) silicate glasses (at a resonance frequency of 79.3 MHz) and Oestrike et al. (1987) did a systematic ^{23}Na MAS NMR study of framework aluminosilicate glasses with varying Si/Al and K/Na ratios (at a higher resonance frequency of 132.2 MHz). Both studies have shown a systematic shift of the peak maximum to higher frequency with increasing K/Na (or Cs/Na) ratio (by about 8–10 ppm) at a given NBO/T and a constant Al/Si ratio. Even at the magnetic field used by Oestrike et al. (1987), there may still be significant quadrupolar broadening, and thus the peak maxima may not correspond to the average δ_i . But as a crude assumption, we may suppose that the peak shifts are mainly caused by changes in the average δ_i , which seems to be the case for sodium silicate glasses discussed above. Hater et al. (1989) pointed out that the shift of the peak maximum with Rb/Na ratio mirrors the change in the electron distribution at the Na site when Na_2O is partially replaced by Rb_2O . However, such an effect is probably too small to cause the observed changes considering the similarity of the alkalis, because (as shown above for the crystals) the shift caused by two more dislike cations (Al^{VI} vs. Ba) is only about 5 ppm. It is likely that the shifts may have an additional

contribution from the first neighbor Na coordination effect. There may also be a slight decrease in the mean Na coordination as a larger network-modifier (K or Rb) is introduced. The introduction of other network modifiers thus seems to have a greater effect on the local coordination environments of Na than does the topology of the tetrahedral network structure. A simple physical scenario of such an interpretation would be that the cation sites have a range of sizes and on average Na occupies the relatively smaller ones, while the larger cation (Rb or K) occupies the larger ones. As the Rb/Na and K/Na ratio increases, Na would on average occupy even smaller sites. An EXAFS study of $\text{Na}_2\text{Si}_2\text{O}_5$ and $\text{Na}_2\text{CaSi}_5\text{O}_{12}$ glasses (Greaves et al. 1981) also suggests that Na in the latter has a higher average coordination, consistent with our interpretation of the NMR results. Our model implies that the network-modifiers are not completely disordered in these glasses. We might expect that as the contrast of the two cations become even larger, greater ordering between the two cations would occur. A recent ^{17}O NMR study of mixed K–Mg silicate glasses have suggested that there is a considerable degree of ordering between K and Mg (Farnan et al. 1992). It is likely that such an ordering would decrease with increasing temperature. It would be interesting to conduct ^{23}Na NMR studies on silicate liquids with mixed network-modifying cations to test this hypothesis.

Conclusions

We have shown that the ^{23}Na chemical shift in anhydrous alkali silicates and aluminosilicates is influenced by several factors including those of the first neighbor anions (Na coordination and mean Na–O bond distance), the bulk polymerization (NBO/T) of the system (which may in essence be an effect of the number of first neighbor network modifiers), and the presence of dissimilar network modifiers (which may also be considered as a first neighbor cation effect). The ^{23}Na δ_i is therefore a useful parameter for studying the local Na coordination environments. Using these relations, we have found that the average Na coordination numbers in anhydrous sodium silicate and aluminosilicate melts of a range of compositions with a single type of network modifier (Na) are 6–7 and vary little with composition. The data also suggest that the average Na coordinations in the melts are insensitive to temperature and thus resemble those of the glasses. ^{23}Na MAS NMR data of glasses of similar compositions provide further evidence that the average Na coordination environments vary little with composition. ^{23}Na MAS NMR data for two series of mixed alkali silicate and aluminosilicate glasses with varying K/Na and Rb/Na ratios show larger changes which may be attributed to changes in the average Na coordination. These limited data may suggest that the local Na coordination environments in silicate glasses are more sensitive to the introduction of other network modifiers than to the topology of the tetrahedral network and warrant further studies on silicate glasses containing mixed cations.

Acknowledgments. We thank Ian Farnan for helpful discussions and for kindly making available a FORTRAN program for the simulations of NMR spectra of quadrupolar nuclei, and Gordon Brown and an anonymous reviewer for useful comments on the manuscript. The study was supported by National Science Foundation grants EAR 89-05188 and EAR 92-04458.

References

- Blundy JD, Wood BJ (1991) Crystal-chemical controls on the partitioning of Ba and Sr between plagioclase feldspar, silicate melts and hydrothermal solution. *Geochim Cosmochim Acta* 55:193–209
- Blundy JD, Wood BJ (1992) Partitioning of strontium between plagioclase and melt: reply to the comment Morse SA (ed). *Geochim Cosmochim Acta* 56:1739–1741
- Brese NE, O'Keeffe M (1991) Bond-valence parameters for solids. *Acta Crystallogr B* 47:192–197
- Brown ID, Altermatt D (1985) Bond-valence parameters obtained from a systematic analysis of the inorganic crystal structure database. *Acta Crystallogr B* 41:244–247
- Buhl J-C, Engelhardt G, Felsche J, Luger S (1988) ^{23}Na MAS-NMR and ^1H MAS-NMR studies in the hydro-sodalite system. *Ber Bunsenges Phys Chem* 92:176–181
- Dal Negro A, De Pieri R, Quarenzi S, Taylor WH (1978) The crystal structures of nine feldspars from the Adamello Massif (Northern Italy). *Acta Crystallogr B* 34:2699–2707
- Dal Negro A, De Pieri R, Quarenzi S, Taylor WH (1980) The crystal structures of nine feldspars from the Adamello Massif (Northern Italy): erratum. *Acta Crystallogr B* 36:3211–3211
- Dallase WA, Thomas WM (1978) The crystal chemistry of silica-rich, alkali-deficient nepheline. *Contrib Mineral Petrol* 66:311–318
- Dirken PJ, Jansen JBH, Schuiling RD (1992) Influence of octahedral polymerization on ^{23}Na and ^{27}Al MAS NMR in alkali fluoroaluminates. *Am Mineral* 77:718–724
- Dupree R, Holland D, McMillan PW, Pettifer RF (1984) The structure of soda-silica glasses: a MAS NMR study. *J Non-Cryst Solids* 68:399–410
- Engelhardt G, Michel D (1987) *High-Resolution Solid-State NMR of Silicates and Zeolites*. Wiley, New York, p 485
- Farnan I, Grandinetti PJ, Baltisberger JH, Stebbins JF, Werner U, Eastman MA, Pines A (1992) Quantification of the disorder in network-modified silicate glasses. *Nature* 358:31–35
- Felsche J, Luger S, Baerlocher C (1986) Crystal structures of the hydro-sodalite $\text{Na}_6[\text{AlSiO}_4]_6 \cdot 8\text{H}_2\text{O}$ and of the anhydrous sodalite $\text{Na}_6[\text{AlSiO}_4]_6$. *Zeolites* 6:367–372
- Greaves GN, Fontaine A, Lagarde P, Raoux D, Gurman SJ (1981) Local structure of silicate glasses. *Nature* 293:611–615
- Gunawardane RP, Cradwick ME, Glasser LSD (1973) Crystal structure of $\text{Na}_2\text{BaSi}_2\text{O}_6$. *J Chem Soc (Dalton)*:2397–2400
- Harlow GE, Brown GE Jr (1980) Low albite: an X-ray and neutron diffraction study. *Am Mineral* 65:986–995
- Hater W, Muller-Warmuth W, Meier M, Frischat GH (1989) High-resolution solid-state NMR studies of mixed-alkali silicate glasses. *J Non-Cryst Solids* 113:210–212
- Hovis GL, Spearing DR, Stebbins JF, Roux J, Clare A (1992) X-ray powder diffraction and ^{23}Na – ^{27}Al – ^{29}Si MAS-NMR investigation of nepheline-kalsilite crystalline solutions. *Am Mineral* 77:19–29
- Jäger C, Barth S, Feltz A (1989) ^{23}Na NMR study of the nasicon system $\text{Na}_{1+x}\text{Zr}_2(\text{PO}_4)_{3-x}(\text{SiO}_4)_x$. *Chem Phys Lett* 154:45–48
- Kirkpatrick RJ (1988) NMR spectroscopy of minerals and glasses. In: Hawthorne FC (ed). *Spectroscopic methods in mineralogy and geology*. Mineralogical Society of America, Washington, D.C., pp 341–403
- Kirkpatrick RJ, Kinsey RA, Smith KA, Henderson DM, Oldfield E (1985) High resolution solid-state sodium-23, aluminum-27, and silicon-29 nuclear magnetic resonance spectroscopic reconnaissance of alkali and plagioclase feldspars. *Am Mineral* 70:106–123
- Kundla E, Samoson A, Lippmaa E (1981) High-resolution NMR of quadrupolar nuclei in rotating solids. *Chem Phys Lett* 83:229–232
- McDonald WS, Cruickshank DWJ (1967) A reinvestigation of the structure of sodium metasilicate, Na_2SiO_3 . *Acta Crystallogr* 22:37–43
- McKeown DA, Waychunas GA, Brown GE Jr (1985) EXAFS and XANES study of the local coordination environment of sodium in a series of silica-rich glasses and selected minerals within the Na_2O – Al_2O_3 – SiO_2 system. *J Non-Cryst Solids* 74:325–348
- Merzbacher CI, White WB (1988) Structure of Na in aluminosilicate glasses: A far infrared reflectance spectroscopic study. *Am Mineral* 73:1089–1094
- Müller D (1982) Zur Bestimmung chemischer Verschiebungen der NMR-Frequenzen bei Quadrupolkernen aus den MAS-NMR-Spektren. *Ann Phys* 39:451–460
- Oestrike R, Yang W-H, Kirkpatrick RJ, Hervig RL, Navrotsky A, Montez B (1987) High-resolution ^{23}Na , ^{27}Al , and ^{29}Si NMR spectroscopy of framework aluminosilicate glasses. *Geochim Cosmochim Acta* 51:2199–2209
- Pant AK (1968) A reconsideration of the crystal structure of β - $\text{Na}_2\text{Si}_2\text{O}_5$. *Acta Crystallogr B* 24:1077–1083
- Pank AK, Cruickshank DWJ (1968) The crystal structure of α - $\text{Na}_2\text{Si}_2\text{O}_5$. *Acta Crystallogr B* 24:13–19
- Phillips BL, Kirkpatrick RJ, Hovis GL (1988) ^{27}Al , ^{29}Si , and ^{23}Na MAS NMR study of an Al, Si ordered alkali feldspar solid solution series. *Phys Chem Minerals* 16:262–275
- Prewitt CT, Burnham CW (1966) The crystal structure of jadeite, $\text{NaAlSi}_2\text{O}_6$. *Am Mineral* 51:956–975
- Stebbins JF, Murdoch JB, Schneider E, Carmichael IS, Pines A (1985) A high-temperature high-resolution NMR study of ^{23}Na , ^{27}Al and ^{29}Si in molten silicates. *Nature* 314:250–252
- Stebbins JF, Farnan I, Williams EH, Roux J (1989) Magic angle spinning NMR observation of sodium site exchange in nepheline at 500°C. *Phys Chem Minerals* 16:763–766
- Stebbins JF, Farnan I (1992) The effects of temperature on silicate liquid structure: a multinuclear, high temperature NMR study. *Science* 255:586–589
- Stebbins JF, Farnan I, Dando N, Tzeng S-Y (1992) Solids and liquids in the NaF - AlF_3 - Al_2O_3 system: a high-temperature NMR study. *J Am Ceram Soc* 75:3001–3006
- Templeman GJ, Van Geet AL (1972) Sodium magnetic resonance of aqueous salt solutions. *J Am Chem Soc* 94:5578–5582
- Vessal B, Greaves GN, Marten PT, Chadwick AV, Mole R, Houde-Walter S (1992) Cation microsegregation and ionic mobility in mixed alkali glasses. *Nature* 356:504–506
- Xue X, Stebbins JF, Kanzaki M, McMillan PF, Poe B (1991) Pressure-induced silicon coordination and tetrahedral structural changes in alkali oxide-silica melts up to 12 GPa: NMR, Raman, and Infrared spectroscopy. *Am Mineral* 76:8–26